Published in final edited form as:
Nat Med. 2012 September ; 18(9): 1401–1406. doi:10.1038/nm.2862.

Galactosylated IgG1 links FcγRIIB and Dectin-1 to block complement-mediated inflammation

Christian M. Karsten[1,*], **Manoj K. Pandey**[2,*], **Julia Figge**[1], **Regina Kilchenstein**[1], **Philip R. Taylor**[3], **Marcela Rosas**[3], **Jacqueline U. McDonald**[3], **Selinda J. Orr**[3], **Markus Berger**[4], **Dominique Petzold**[4], **Veroniqué Blanchard**[4], **André Winkler**[5], **Constanze Hess**[5], **Delyth M. Reid**[6], **Irina V. Majoul**[7], **Richard T. Strait**[8], **Nathaniel L. Harris**[2], **Gabriele Köhl**[1], **Eva Wex**[9], **Ralf Ludwig**[10], **Detlef Zillikens**[10], **Falk Nimmerjahn**[11], **Fred D. Finkelman**[2,12,13], **Gordon D. Brown**[6], **Marc Ehlers**[1,5], and **Jörg Köhl**[1,2]

[1]Institute for Systemic Inflammation Research, University of Lübeck, 23538 Lübeck, Germany

[2]Divisions of Cellular and Molecular Immunology, Cincinnati Veterans Affairs Medical Center Cincinnati, Ohio 45229, USA

[3]Institute of Infection and Immunity, Cardiff University School of Medicine, Heath Park, Cardiff CF14 4XN, UK

[4]Glycodesign and Glycoanalytics, Central Institute of Laboratory Medicine and Pathobiochemistry, Charité Medical University, 10117 Berlin, Germany

[5]Laboratory of Tolerance and Autoimmunity, German Rheumatism Research Center (DRFZ), 10117 Berlin, Germany

[6]Section of Infection and Immunity, University of Aberdeen, Aberdeen AB25 2ZD, U.K

[7]Institute of Biology, Center for Structural and Cell Biology in Medicine, University of Lübeck, 23538 Lübeck, Germany

[8]Emergency Medicine, Cincinnati Veterans Affairs Medical Center Cincinnati, Ohio 45229, USA

[9]Department of Respiratory Diseases Research, Boehringer Ingelheim Pharma GmbH &Co. KG, 88397 Biberach, Germany

[10]Department of Dermatology, University of Lübeck, 23538 Lübeck, Germany

[11]Department of Biology, Chair of Genetics, University of Erlangen-Nuremberg, 91058 Erlangen, Germany

[12]Division of Immunology, University of Cincinnati College of Medicine, Cincinnati Veterans Affairs Medical Center Cincinnati, Ohio 45229, USA

[*]These authors contributed equally to this work

Author information. Eva Wex is an employee of Boehringer Ingelheim Pharma GmbH & Co. KG.

Author contributions. C.M.K and M.K.P. conducted key studies and analyzed the data. J.F. assessed antigen binding of in vitro glycosylated IgGs, performed phenotypical characterization of BM cells and some in vivo studies. R.K. and C.M.K. performed the epidermolysis bullosa acquisita (EBA) studies. R.F. and D.Z. provided the rabbit anti-collagen type VII IgG for the EBA studies and helped with EBA-related data analysis. P.R.T., M.R. and J.U.M. provided the Dectin-1-transduced neutrophil and macrophage cell lines and helped with assays using such lines. S.J.O. performed the peptide pull-down experiments. M.B., D.P. and V.B. did the MALDI-TOF analysis. A.W. and C.H. performed the in vitro galactosylation of the H5 Ab. G.D.B. and D.M.R. provided the *Clec7a*$^{-/-}$ mice and helped with the neutrophil assays using such mice and with ex vivo assays with primary *Clec7a*$^{-/-}$ cells. I.V.M. provided precious material and invaluable advice for the FRET experiments. T.S. and F.D.F. provided TNP-OVA and helped with initial IC studies. N.L.H. and G.K. performed the ERK phosphorylation studies with neutrophils. E.W. provided the conditional Syk knockout mice and the protocol for in vitro Syk depletion. F.N. provided the recombinant IgG1 7B4 Ab, soluble FcγRIIB and assessed HiGalH5- and H5-IC binding to FcγRIIB-transfected CHO cells. M.E. provided scientific input and coordinated the glycan analysis. J.K. designed and coordinated the study, analyzed the data and wrote the manuscript.

Europe PMC Funders Author Manuscripts

[13]Department of Medicine, Cincinnati Veterans Affairs Medical Center Cincinnati, Ohio 45229, USA

Abstract

Complement is an ancient danger sensing system playing critical roles in host defense, immune surveillance and homeostasis[1]. C5a and its G-Protein-coupled receptor mediate many of the pro-inflammatory properties of complement[2]. Despite its critical role in allergic asthma[3], autoimmune arthritis[4], sepsis[5] and cancer[6], our knowledge about C5a regulation is limited. Here we demonstrate an unexpected link through which IgG1 immune complexes (IC), the inhibitory IgG receptor FcγRIIB and the C-type lectin-like receptor Dectin-1 suppress C5a receptor (C5aR) functions. Specifically, we found that IgG1 IC associate FcγRIIB with Dectin-1, resulting in phosphorylation of spleen tyrosine kinase (Syk) downstream of Dectin-1 and Src homology 2 domain containing inositol phosphatase (SHIP) downstream of FcγRIIB. This pathway blocks C5a receptor-mediated ERK1/2 phosphorylation and C5a effector functions *in vitro* and C5a-dependent inflammatory responses *in vivo* including the development of skin blisters in experimental epidermolysis bullosa acquisita (EBA), an autoimmune skin disorder. Notably, high galactosylation of IgG N-glycan is critical for this inhibitory property of IgG1 IC as it promotes the association between FcγRIIB and Dectin-1. Thus, galactosylated IgG1 and FcγRIIB exert immunoregulatory properties beyond their impact on activating FcγRs that may control allergy, autoimmunity and cancer.

The inflammatory responses in experimental autoimmune nephritis[7,8], arthritis[9], IC alveolitis[10] and peritonitis[11] are mediated by activating FcγRs and C5aR. The emerging paradigm is that C5a decreases the cellular activation threshold by upregulation of the ratio between activating and inhibitory FcγRs (known as the A/I ratio)[10,11], whereas activating FcγRs eventually drive the pro-inflammatory effector functions[12]. However, C5a recruits and activates inflammatory cells such as neutrophils, macrophages and mast cells independent of FcγRs[2]. FcR γ-chain deficient (*Fcer1g*$^{-/-}$) mice express no functional activating FcγRs but do express the inhibitory FcγRIIB. They are protected from IC-mediated inflammation despite the presence of C5a. We hypothesized that one mechanism underlying such protection could be an anti-inflammatory property of IgG IC suppressing C5a-mediated effector functions.

To test our hypothesis, we injected C5a into the peritoneal cavity of BALB/c (WT) or *Fcer1g*$^{-/-}$ mice. As expected, we observed strong neutrophil recruitment in both mouse strains (Fig. 1a). IgG1 is the most abundant isotype of serum antibody (Ab) in mice. The preferential binding of IgG1 to inhibitory FcγRIIB is considered a protective mechanism to prevent incidental activation of circulating myeloid cells by binding of IC to activating FcγRs[12]. Intravenous injection of IC comprising the anti-TNP-IgG1 clone 107.3 and TNP-OVA (107.3 IC)[13] 30 min prior to C5a administration reduced the C5a-mediated neutrophil migration into the peritoneum in wt and *Fcer1g*$^{-/-}$ mice but not in *Fcgr2b*$^{-/-}$ mice **(**Fig. 1a **and** Supplementary Fig.1**)**. We found no anti-inflammatory effect for monomeric 107.3-Ab (data not shown). Further, 107.3-IC blocked IC-peritonitis[11] in WT but not in *Fcgr2b*$^{-/-}$ mice, demonstrating a critical role of FcγRIIB for 107.3 IC-mediated inhibition of C5a-dependent inflammation **(**Fig. 1b**)**.

The mechanisms leading to C5aR-mediated extravasation and tissue recruitment of neutrophils involve the β2 integrin CD11b/CD18 (CR3)[14]. C5a dose-dependently upregulated CD11b expression on neutrophils from WT (data not shown) and *Fcer1g*$^{-/-}$ mice **(**Supplementary Fig. 2**)**, which was significantly reduced upon 107.3-IC treatment. This reduction was absent with cells from *Fcgr2b*$^{-/-}$ mice **(**Fig. 1c**)**. Further, 107.3-IC administration reduced C5a-dependent neutrophil adhesion with cells from *Fcer1*$^{-/-}$ but not

from *Fcgr2b*$^{-/-}$ mice **(**Fig. 1d**)**. Next, we assessed the impact of 107.3 IC on C5a-mediated chemotaxis **(**Supplementary Figs. 3a, d**)** and found a dose-dependent inhibition of C5a-mediated chemotaxis with BM neutrophils and peritoneal macrophages **(**Fig. 1e **and** Supplementary Fig. 3c,d**)** from WT and *Fcer1g*$^{-/-}$ but not from *Fcgr2b*$^{-/-}$ mice. Further, pharmacological targeting of FcγRIIB abrogated the inhibitory effect of 107.3-IC **(**Supplementary Fig. 4**)**. Thus, 107.3-IC not only inhibit the functions of activating FcγRs[12] but also of complement-mediated acute inflammation.

In addition to C5aR, we found that 107.3-IC completely blocked CXCL2-dependent neutrophil migration of wt and *Fcer1g*$^{-/-}$ but not of *Fcgr2b*$^{-/-}$-derived cells **(**Supplementary Figs. 3b, e**)** suggesting a more general mechanism of inhibition.

C5aR exerts many of its biological functions through activation of mitogen-activated protein (MAP) kinases involving extracellular signal-regulated kinases 1/2 (ERK1/2) and the phospholipase C/inositol phosphate pathway leading to an increase in intracellular calcium release ($[Ca^{2+}]_i$)[2]. 107.3-IC blocked C5a-mediated rise of $[Ca^{2+}]_i$ in BM-cells from WT and *Fcer1g*$^{-/-}$mice but not from *Fcgr2b*$^{-/-}$ mice **(**Figure 1f**)**. Further, C5a drove phosphorylation of ERK1/2 in Gr1$^+$ BM-neutrophils **(**Supplementary Fig. 5a**)** and 107.3-IC dose-dependently inhibited this ERK1/2 activation in BM-neutrophils from WT but not from *Fcgr2b*$^{-/-}$ mice **(**Fig. 1g **and** Supplementary Fig. 5b**)**. This inhibitory effect was similar to what we found when C5aR signalling was blocked with a C5aR antagonist **(**Fig. 1h**)**. Taken together, these results demonstrate that IgG1-IC block C5a-mediated inflammation by an FcγRIIB-dependent mechanism that inhibits ERK1/2 phosphorylation and the phospholipase C/inositol phosphate pathway.

FcγRIIB negatively regulates cell activation through an immunoreceptor tyrosine-based inhibitory motif (ITIM) that becomes phosphorlyated upon pairing with the immunoreceptor tyrosine-based activation motif (ITAM) downstream of activating FcγRs by an Src family kinase-dependent mechanism[12]. The tyrosine-phosphorlyated ITIM then allows binding and activation of SHIP. Because 107.3-IC block C5a-mediated chemotaxis of myeloid cells from *Fcer1g*$^{-/-}$ mice, the effect does not result from classical pairing of activating FcγRs with FcγRIIB. In search for potential new partners of FcγRIIB driving ITIM and SHIP phosphorylation, we focused on Dectin-1 (gene symbol *Clec7a*), as it harbors an ITAM-like motif and is expressed on neutrophils[15]. First, we evaluated the impact of the Dectin-1 inhibitor laminarin and the Dectin-1 agonist curdlan on the inhibitory effect of 107.3-IC. Laminarin treatment significantly reduced whereas preincubation with curdlan largely blocked the 107.3-IC inhibitory effect on C5a-mediated neutrophil migration, indicating that Dectin-1 is critical **(**Fig. 2a**)**. Notably, the particulate ß-glucan polymer curdlan but not the soluble polymer laminarin promotes rapid internalization of Dectin-1[16] **(**Supplementary Fig. 6**)** suggesting that the surface availability of Dectin-1 is crucial for the IgG1-IC effect. We found that 30-40% of Ly-6G^{hi} neutrophils express Dectin-1. C5aR expression follows the same pattern, i.e. about 25-30% of the Ly6G^{hi} neutrophils express Dectin-1and C5aR. About 10% of BM-neutrophils are C5aR^{dim}Dectin-1^{neg}. FcγRIIB is expressed on almost all Ly-6G^{hi} neutrophils **(**Fig. 2b**)**. In line with these findings, only Ly6G^{hi}Dectin-1$^+$C5aR$^+$ neutrophils migrated towards C5a **(**Fig. 2c**)**. Further, 107.3-IC failed to inhibit C5a-mediated migration of neutrophils from *Clec7a*$^{-/-}$ mice[17] **(**Fig. 2d**)** and C5a-mediated migration was blocked in *Clec7a*$^{-/-}$ neutrophils, retrovirally transduced with the Dectin-1B isoform but not with the control vector lacking Dectin-1[18] **(**Fig. 2e **and** Supplementary Fig. 7**)**. Thus, IgG1-IC require FcγRIIB and Dectin-1 to inhibit C5a-mediated effector functions in neutrophils.

In search of signalling pathways underlying this inhibitory effect of IgG1-IC, we noted that the inhibitory effect already occurred after one min and that inhibition of tyrosine phosphorylation by genistein completely abrogated the IgG1-IC effect **(**Supplementary Fig.

8a **and** Fig. 3a**).** pSrc-kinases mediate tyrosine phosphorylation of the FcγRIIB-associated ITIM and the ITAM-like motif in Dectin-1. We found that the two Src-family kinase inhibitors I and II completely blocked the inhibitory effect of 107.3-IC **(**Figs. 3b, c**)**.

Dectin-1 ligation promotes a signalling pathway that results in the phosphorylation of Syk[19]. Notably, genetic deletion of Syk in inducible Syk-deficient mice[20] and pharmacological targeting by the four different Syk kinase inhibitors R406, piceatannol, BAY 61-3606 or Syk inhibitor IV completely reversed the inhibitory effect of IgG1-IC on C5a-mediated neutrophil chemotaxis **(**Fig. 3d,e **and** Supplementary Figs. 8b-d **and** 9**)**. Further, we pulled down p-Syk with a Syk-binding phosphopeptide[21] in the *Clec7a*$^{-/-}$ neutrophil cell line transduced with the Dectin-1B isoform following 107.3-IC treatment **(**Supplementary Fig. 8e**)**. Finally, we show Syk and SHIP phosphorylation in neutrophils from wt but not from *Fcgr2b*$^{-/-}$ or *Clec7a*$^{-/-}$ mice in response to 107.3-IC treatment by confocal microscopy. These studies further demonstrate co-localization of p-Syk or p-SHIP with FcγRIIB and Dectin-1 in response to 107.3-IC administration **(**Fig. 3f,g **and** Supplementary movies 1-5**)**. Notably, 107.3-IC treatment resulted in rapid and transient Syk and SHIP phosphorylation within 1-3 min that declined after 5 min **(**Supplementary Fig. 10a,b**)**.

Taken together, these data suggest that IgG1-IC engage Dectin-1 leading to Syk phosphorylation. Further, our data indicate that tyrosine and Syk phosphorylation downstream of Dectin-1 are linked to tyrosine phosphorylation of the ITIM within FcγRIIB and subsequent SHIP phosphorylation. This pathway then blocks C5a-mediated ERK1/2 phosphorylation and the phospholipase C/inositol phosphate pathway critical for C5a-mediated pro-inflammatory effector functions.

To identify the mechanism underlying the interaction of IgG1-IC with Dectin-1 and FcγRIIB, we focused on the Fc glycan composition. The N-glycan at Asn^{297} of the Fc moiety is critical for IgG binding to FcγRs[22], the serum collectin mannose-binding lectin (MBL)[23] and the collectin-related molecule C1q[24]. Dectin-1 recognizes ß-1,3 glucans expressed by a broad range of fungal pathogens[25]. However, no interaction with any Fc glycan has been reported. When we determined the N-glycan composition **(**Supplementary Fig. 11**)** of 107.3-Ab by matrix-assisted laser desorption/ionization time-of-flight mass spectroscopy (MALDI-TOF), we observed 81% glycan galactosylation. We further determined the N-glycan composition of the two TNP-specific IgG1 antibodies 7B4 and H5[27]. Galactosylation was only 25.1% or 30.3% **(**Supplementary Fig. 12, Supplementary table**)**. IgG1-IC generated with 7B4- or H5-Ab did not inhibit C5a-mediated chemotaxis of BM-neutrophils **(**Supplementary Fig. 13a**)**. To directly assess the importance of N-glycan galactosylation, we galactosylated or degalatcosylated H5-Ab *in vitro* resulting in HiGalH5-Ab and LoGalH5-Ab. Glycan remodelling had no effect on antigen binding **(**Supplementary Fig. 14**)**. HiGal- but not LoGalH5-IC inhibited C5a-mediated chemotaxis, CD11b upregulation and increase in $[Ca^{2+}]_i$ with neutrophils from WT and *Fcer1g*$^{-/-}$ but not from *Fcgr2b*$^{-/-}$ or *Clec7a*$^{-/-}$ mice **(**Supplementary Figs. 13a-c**)**. Additional sialylation of highly galactosylated H5-Ab did not alter the inhibitory effect. Notably, highly galactosylated anti-TNP IgG2a-IC did not block C5a-mediated chemotaxis *in vitro* **(**Supplementary Fig. 15a-c**)**.

In vivo, HiGal- but not LoGalH5-IC almost completely suppressed C5a-mediated neutrophil recruitment into the peritoneum of WT but not of in *Fcgr2b*$^{-/-}$ or *Clec7a*$^{-/-}$ mice **(**Fig. 4a**)**. Further, intravenous administration of curdlan resulted in internalization of Dectin-1 in migrated neutrophils and abrogated the blocking effect of HiGalH5-IC on C5a-mediated peritoneal inflammation **(**Fig. 4b **and** Supplementary Fig. 16**)**. Previous data suggest a critical role for C5 in an experimental model of EBA[28], a subepidermal autoimmune blistering disease. We found that C5aR$^{-/-}$ mice were protected from EBA development **(**Supplementary Fig.17**)**. In line with this finding, HiGalH5-IC but not LoGalH5-IC

treatment resulted in a significant reduction of the cutaneous lesions **(**Figs. 4c,d **and** Supplementary Fig. 18**)**. HiGal-IC had not protective effect in *Clec7a*$^{-/-}$ mice confirming the importance of Dectin-1 in this model **(**Supplementary Fig. 19**)**. Notably, Dectin-1-deficient patients or mice do not develop spontaneous autoimmunity. However, our data suggest that Dectin-1 may aggravate the inflammatory effector response in autoimmune diseases mediated by C5a. In line with this view, data from experimental autoimmune arthritis[29] and encephalitis models[30] point toward a role for Dectin-1 as a modulator of autoimmune-driven inflammation.

Finally, we show by Förster resonance energy transfer (FRET) that HiGalH5- but not LoGalH5-IC associate with Dectin-1. In addition, we found that in the absence of FcγRIIB, IgG1 IC do not bind to Dectin-1 independent of their galactosylation status **(**Fig. 4e-g **and** Supplementary Figs. 20-22**)**.

Collectively, our findings demonstrate that high N-glycan galactosylation of IgG1 molecules promotes cooperative signalling of the FcγRIIB with Dectin-1 resulting in an inhibitory signalling pathway that blocks pro-inflammatory effector functions of the chemoattractant GPCRs C5aR and CXCR2 **(**Supplementary Fig. 23**)**. This mechanism is distinct from the anti-inflammatory properties mediated by sialylation of Fc-linked N-glycans[31]. About 25-35% of Fc glycans from serum IgG are agalactosylated under steady state conditions. This frequency markedly increases in experimental and human autoimmune conditions including rheumatoid arthritis, systemic lupus erythematosus, inflammatory bowel disease as well as in infections[32]. Thus the inhibitory effect of highly galactosylated IgG1 IC may serve as a feedback loop to control complement and chemokine-mediated inflammation in autoimmunity and infection before IgGs switch to the harmful agalactosyl glycoform. This effect may also contribute to the increased incidence of autoimmune phenomena in patients with hypogammaglobulinemia or common variable immunodeficiency[33].

Methods

Reagents

Monoclonal PE-labelled Abs to CD11b (M1/70), Ly-6G (1A8) and Gr-1 (RB6-8C5) were from BD Pharmingen; Alexa488-labelled FcγRIIB-specific Ab (Ly17.2) was used as described[11]; Monoclonal Abs to F4/80 (Cl:A3-1), Ly-6B.2-FITC (7/4), Dectin-1-APC or Alexa647 (2A11) and CD88 PE or Alexa647 (10/92) were from AbD Serotec. The Alexa647 Ab to TLR4 (MTS510) was from eBioscience. The Abs to F4/80 and Ly-6B.2 were labelled with Phycolink Peridinin-chlorophyll-protein complex (PerCP)-labelling kit (Europa Bioproducts) as per manufacturer's instructions; the rabbit Abs to anti phospho-p44/42 MAPKinase (# 9101), phospho-Syk (Tyr352), phospho SHIP1 (Tyr1020), IgG HRP and anti-pSyk (C87C1) were from Cell Signaling; the Ab to Syk was from Novus Biologicals. Streptavidin-Alexa Fluor 405 (SAv-Alexa405), TSA detection kit Alexa Fluor 546, Fluo-4-AM and zeocin were from Invitrogen. The FITC-labeled pig Ab to rabbit IgG was from Dako. Diff-Quick staining solution was from Baxter, Merz & Dade. The goat Ab to C3 Ab was from MP Biomedicals. The C5a receptor antagonist A8$^{\Delta 71\text{-}73}$ has been described elsewhere[34]. The mouse TNP-specific IgG Ab 107.3 was from BD Pharmingen. The mouse TNP-specific IgG1Ab 7B4 was generated by switching the original TNP-specific IgG2a Ab to IgG1 and was produced by transient transfection in HEK293 cells as described[27]. The TNP-specific mouse IgG2a 7B4 Ab was produced from hybridoma cells. Recombinant human C5a (rhC5a), Calcein, 4-hydroxytamoxifen as well as genistein, piceatannol and R406 were from Sigma-Aldrich. The Src kinase inhibitors I and II, Syk inhibitors IV and BAY 61-3606 were from Calbiochem. Poly-L-lysine coated microtiter plates were from Corning. Laminarin, curdlan, SCF and ß-estradiol were from Sigma-Aldrich. IL-3 and IL-6 were from Peprotec. Mouse FcγRIIB-Fc and CHO-mFcγRIIB were

used as described[35]. TNP^9-coupled BSA was from Biosearch Technology. Supplemented RPMI 1640 medium was from PAA laboratories. Fluoromount-G was from SouthernBiotech. Cy3 Amersham CyDye™ Antibody Labeling Kit was from GE Healthcare. The PVDF membrane was from Millipore.

Animals

Female BALB/c or C57BL/6 mice were purchased from the Jackson Laboratory (Bar Harbor ME). *Fcer1g*$^{-/-}$ and *Fcgr2b*$^{-/-}$ mice (on BALB/c background) were purchased from Taconic (Laven, Denmark). Dectin-1-deficient mice on the isogenic 129S6/SvEv (129S6/SvEv.*Clec7a*$^{-/-}$), the C57BL/6 (C57BL/6.*Clec7a*$^{-/-}$), the 129S6/SvEv and the C57BL/6 control animals were obtained from our own breeding colonies. Dectin-1-deficiency was also backcrossed for 8 generations onto the C57BL/6 genetic background for the production of cell lines (see below). C57BL/6.*Clec7a*$^{-/-}$ mice were used in peritonitis and in chemotaxis experiments with naive H5, HiGal- and LoGalH5-IC. Inducible Syk knockout mice have recently been described[20] and were bred at Charles River. All animals were used at 8-12 weeks of age and handled in accordance with the appropriate Institutional and National guidelines. All animal studies were reviewed and approved by local authorities of the Animal Care and Use Committee (Ministerium für Landwirtschaft, Umwelt und ländliche Räume, Kiel, Germany) and performed by certified personnel.

Chemotaxis assay

BM-derived cells or peritoneal macrophages were resuspended in chemotaxis medium (GBSS containing 2% BSA) at a density of 5×10^6 cells ml^{-1}. The chemoattractants C5a (10^{-8} M) or CXCL2 (10^{-7}M) were diluted in chemotaxis medium, placed in the bottom wells of a micro Boyden chemotaxis chamber (Neuroprobe) and overlaid with a 3 μm polycarbonate membrane. Then, 50 μl of the cells were placed in the top wells and incubated for 30 minutes at 37°C. In some experiments, cells were treated with the indicated concentrations of monomeric IgG1 or IgG1-IC, IgG2a-IC, the tyrosine phosphorylation inhibitor genistein (100μM), the src family kinase inhibitors I and II (at 10 μM), or the Syk inhibitors piceatannol (100μM), R406 (10 μM), Syk inhibitor IV (10 μM) or BAY 61-3606 (10 μM). Subsequently, the membranes were removed and the cells on the bottom side of the membrane were stained with Diff-Quick. The numbers of migrated cells in five high-power fields were counted and the number of cells per mm^2 was calculated by computer assisted light microscopy. Results are expressed as the mean value of triplicate samples.

Preparation of TNP-OVA and of TNP-OVA anti-TNP-OVA IgG1 immune complexes

TNP-OVA complexes were generated as described[13]. Briefly, one gram of OVA was dissolved in 5 ml of saline and mixed with 500 μl 1M $NaHCO_3$ pH 9.6. Then 50mg of TNP-OSU were dissolved in 500μl DMSO resulting in 100 mg/ml^{-1} TNP-OSU, which was added to the OVA solution and incubated overnight. The final TNP/OVA ratio was 10.4. TNP-OVA complexes were incubated with TNP-specific IgG1 Abs at different ratios and IC formation was determined by Ouchterlony gel diffusion.

C5a-mediated peritoneal inflammation

Mice were injected with C5a (200 nM, 100 μl, i.p.). After six h, mice were sacrificed, and neutrophil numbers in peritoneal lavage fluid were determined by Diff-Quick staining of cytospin slides. At least >20 different microscopic fields were evaluated as described[11]. In some experiments, Ly-$6G^{hi}$ neutrophil numbers were enumerated by flow cytometry using BD True count beads. In some experiments, mice were pretreated i.v. with 107.3 IC (0.5 – 50 μg kg^{-1} body weight), HiGal- or LoGalH5-IC (50 μg kg^{-1} body weight).

Immune complex peritonitis

We used the model of a reversed passive Arthus reaction. Ovalbumin (OVA, 20 mg/kg body weight; Sigma) was injected i.v., followed by an i.p. injection of OVA-specific rabbit IgG (800 μg/mouse; ICN) as described[11]. Briefly, mice were sacrificed 6 h after injury and the peritoneal cavity was lavaged with 10 ml of PBS. Peritoneal cells were washed once with PBS and 10^5 cells in 200 μl of PBS were used for preparation of cytospin slides. Neutrophil numbers were evaluated as outlined above. In some experiments, mice were pretreated i.v. with 107.3-IC at a concentration of 50 μg kg^{-1} body weight.

Generation and purification of pathogenic anti-type VII collagen antibodies

Rabbits were immunized with recombinant forms of the NC1 domain of murine type VII collagen as described[28]. IgG from immune and normal rabbit sera were purified by affinity chromatography using protein G affinity as previously reported[28]. Isolated IgG was further subject to affinity purification using recombinant His-tagged fragments of murine type VII collagen (amino acids 757-967) and Affi-Gel affinity chromatography (BioRad Lab). Reactivity of the isolated IgG fractions was confirmed by immunofluorescence microscopy on murine skin before *in vivo* use.

Experimental EBA model

Induction of experimental EBA followed published protocols[28] with minor modifications. Briefly, EBA was induced by a total of three s. c. injections of 100 μg rabbit anti-type VII collagen affinity-purified IgG every 2nd day. For treatment, i.v. injections of either PBS, HiGal-, LoGalH5 or 107.3-IC were started on day -1 and repeated on days 3 and 6. Disease progression was evaluated over a time period of 12 d. On d 4, 7 and 12, disease severity was determined, expressed as percent of body surface area affected by skin lesions and tail biopsies were taken. On d 12, additional tissue samples were obtained for histological analyses. Disease outcome of the different treatment groups was compared by calculation of the area under the curve (AUC) obtained for the disease progression at the different time points, taking both disease onset and maximal disease activity into account.

Histopathology and immunofluorescence microscopy

Tissue samples were used for histopathological assessment and immunofluorescence microscopy as described previously[28]. To assess morphological skin alteration in diseased mice, sections were stained with hematoxylin and eosin. IgG and C3 deposits were detected by direct immunofluorescence microscopy using a FITC-labeled pig anti-rabbit IgG Ab and goat anti-mouse C3 Ab.

Neutrophil preparation

Mice were killed by cervical dislocation under anesthesia. Femurs, tibias and humeri were removed, placed in PBS on ice and subsequently flushed with PBS. More than 80% of cells isolated were polymorphonuclear cells as defined by Diff-Quick staining and stained positive for the Ly-6G marker. For Syk depletion in neutrophils from $Syk^{flox/flox}$ mice, cells were cultured in RPMI 1640 medium supplemented with 2 mM L-Glutamine, 100 U/ml benzylpenicillin / 0.1 mg/ml dihydrostreptomycin (Pen/Strep) and 10% FCS in the presence 0.6 μM 4-hydroxy-tamoxifen in ethanol for 48 h. Controls were treated accordingly with ethanol only. Viability was determined by trypan blue exclusion and 7AAD staining using a BD LSR II flow cytometer. Forty-eight hours treatment with 4-hydroxy-tamoxifen did not affect the viability of BM neutrophils.

Macrophage preparation

To obtain mouse peritoneal macrophages, the peritoneal cavity was gently flushed with 5 ml of sterile PBS. PE cells were allowed to adhere on plastic microtiter plates for 4 h at 37°C. Non-adherent cells were removed by several washing steps with PBS and adherent cells were used for cell migration. Flow cytometric analysis revealed that the majority of adherent cells were F4/80^{high} CD11b^{high}.

C5a-induced upregulation of CD11b expression

Neutrophils (1×10^6) were suspended in 100ul of GBSS buffer containing 2%BSA and treated with C5a (10nM) at 37°C for 10 min. Then, cells were placed on ice and washed once with ice-cold PBS. For flow cytometric analysis of CD11b expression, Fc receptors were blocked with 2.4G2 Ab (1 μg/10^6 cells in 100 μl of FACS buffer for 30 min on ice). Cells were washed once with PBS and then stained with anti-CD11b Ab conjugated to PE or the corresponding isotype control for 45 minutes on ice. Data were collected and analyzed on a FACSCalibur (Becton Dickinson) using FCSExpress software (Version 3.0).

Complement receptor 3-mediated cell adhesion assay

Complement (iC3b)-coated surfaces were prepared by incubation of poly-L-lysine pre-coated plates with human IgM (10 μg ml^{-1}) and 10% human serum as described[36]. BM cells were labeled with calcein (2 μg ml^{-1}) for 30 min and added to the complement-coated surface ± C5a (0.1, 1 or 10×10^{-9}M) for 10 min at 37°C. In some experiments, calcein-labeled cells were preincubated with 107.3-IC (0.1 or 1 μg ml^{-1}) for 30 min at 37°C. The fluorescence was measured using an FLX800 Microplate Fluorescence Reader (BioTek Instruments Inc) before and after washing twice with PBS. The percent adhesion was calculated by dividing the fluorescence signal remaining after washing by that observed before washing.

Increase in intracellular calcium $[Ca^{2+}]_i$

BM cells were collected and loaded with 5μM of the Ca^{2+}-sensitive fluorophore Fluo-4-AM (Invitrogen) for 30 minutes. Non-incorporated dye was washed away using PBS. Cells were then gated on Ly-6G^{hi} cells and analyzed on an LSRII flow cytometer (BD). The background signal was recorded for 30 sec. Then C5a was added (10 nM) and recording was continued for another 90 sec. The increase in $[Ca^{2+}]_i$ was calculated by assessment of the Ca^{2+} peak using the kinetic plug-in tool of the FlowJo software (Ver. 7.5, Tree Star Inc.).

Analysis of ERK1/2 phosphorylation

BM cells from wt mice were cultured ± 107.3–IC (0.1 or 1 μg ml^{-1}) or the C5aR antagonist A8$^{\Delta 71\text{-}73}$ for 30 min at 37°C. BM cells were then stimulated with C5a (50 nM) for 1 min and subsequently analyzed for ERK1/2 phosphorylation by intracellular staining with a rabbit anti-phospho-p44/42 MAPKinase Ab. In some experiments, BM cells from *Fcgr2b*$^{-/-}$ mice were used.

In vitro generation of neutrophils

BM cells were pooled from the femurs of female C57BL/6.*Clec7a*$^{-/-}$ mice and were depleted of lineage (lin)$^+$ cells using the MACS murine lineage depletion kit (Miltenyi) as directed by the manufacturer. The lin$^-$ cells were prestimulated with IL-3, IL-6 and SCF for 3 days as described[37] before being infected with the pMXs-IP:FL-ER-Hoxb8 retrovirus[18] and then immediately cultured in SCF and β-estradiol to bias towards neutrophil progenitor outgrowth. Two days after infection cells were selected in 1.5 μg/ml of puromycin for 10 d. Typically this resulted in the production of stable precursors, termed Myeloid Precursor Hoxb8 from C57BL/6 (MyPH8-B6). The cells were maintained in SCF and β-estradiol as

described[37]. MyPH8-B6.*Clec7a*$^{-/-}$ cells were reconstituted with the dectin-1B isoform with specific (pMXs-IZ:dectin-1B) or empty control (pMXs-IZ) retrovirus as previously described[38], but using MyPH8 culture medium supplemented with 50 μg/ml of zeocin to maintain the reconstituted cells. Expression of dectin-1B was verified by flow-cytometry. For *in vitro* generation of neutrophils, MyPH8-B6.*Clec7a*$^{-/-}$:pMXs-IZ or MyPH8-B6.*Clec7a*$^{-/-}$:Dectin-1B were washed 3 times with media to remove the β-estradiol prior to differentiation for 4 d in SCF and G-CSF (both 20 ng ml^{-1}). By day 4, neutrophils routinely represent 90-98% of the cells present and are identified by flow-cytometry as Ly-6B.2^{high}CD117^{low} cells and on cytospin preparations by their typical nuclear morphology.

Peptide pull-down and western blotting

The cells were serum starved for 30 min at 37°C. Ten million were resuspended in 100 μl DPBS and stimulated at 37°C with 10μg IgG1-IC for the indicated times. Cells were lysed with RIPA lysis buffer (50 mM Tris-HCl pH7.4, 150 mM NaCl, 1% IGEPAL-CA-630, 0.25% Na-Deoxycholate, 1mM EDTA, Na_3V0_4, leupeptin, aprotinin and phenylmethylsulfonyl fluoride). For peptide pull-down experiments using a previously described biotinylated phospho-peptide[21] derived from Clec-2 (pClec2: MQDEDGpYITLNIKNK-biotin, Peptide Protein Research Ltd), cell lysates were incubated with 20 μg of peptide bound to Streptavidin agarose beads (Life Technologies) for 4 h. Peptide pull-downs were washed, reducing Laemmli buffer was added and samples were heated for 5 min at 95°C. Samples were separated by SDS-PAGE, transferred to PVDF membrane and analyzed by Western blot using anti-pSyk and anti-Syk antibodies.

Immunofluorescence staining of BM neutrophils

Neutrophils were preincubated for different time periods (1, 3, 5 min) with or without IgG1-IC at 37°C. Cells were then fixed with BD Cytofix/Cytoperm (BD Bioscience). Phospho-Syk or phospho-SHIP Abs were added and the cells were incubated at 4°C for 24h. Cells were washed and then stained for phospho-Syk detection with an Alexa-568 labeled secondary Ab, or, in case of SHIP, using the tyramide signal amplification kit as described by the manufacturer. For FcγRIIB and Dectin-1 staining, samples were further incubated with Alexa488-labled FcγRIIB and/or APC-Dectin-1-specific Abs for 15 min at 4°C. Cells were then mounted with Fluoromount-G. Images were obtained using the Olympus FV 100 confocal microscope (Olympus, Germany) with a 60x- NA:1.35 oil objective. Image analysis and capturing was performed using the Fluoview 2.1c software.

3-D Image analysis

Z-stacks were taken with an interval of 0.1 μm using a the Olympus FV 1000 confocal microscope (Olympus, Germany) with 20 to 30 slices per stack in order to show cells in their full extension. Stacks were then used for image analysis by IMARIS software (version 7.0.1.1, Bitplane AG, Switzerland), operating with IMARIS Surpass (volume and isosurfaces rendering analysis) to visualize and locate points of interest (e.g. FcγRIIB, Dectin-1 and p-Syk expression). For co-localization studies, data sets were analyzed using the IMARIS software.

Surface Plasmon Resonance Analysis (SPR)

To determine the interactions between FcγRIIB with HiGal and LoGal H5 IC, SPR was performed using a Biacore 3000 (GE Healthcare) system at 25°C. FcγRIIB was coupled to the CM5 sensor chip (GE Healthcare) via amine coupling. For activation of the carboxylated dextran matrix of the CM5 chip, 0.05 M N-hydroxysuccinimide and 0.2 M N-ethyl-N'-(dimethylamino-propyl) carbodiimide in equal volumes were added to the sensor chip. For immobilization, FcγRIIB was diluted to 34 μg ml^{-1}. Injection of 5 μl receptor resulted in

signal increase of 6000 resonance units (RU). Unbound reactive groups were saturated with 1 M ethanolamine hydrochloride-NaOH for 7 min. A second flow chamber was subjected to the immobilization protocol but without any addition of protein and served as a reference cell. Serial dilutions of HiGalH5- or LoGalH5-IC in PBS were added (starting at 10 nM). For detection of association, the samples were passed over the sensor chip at a constant flow rate of 15 μl min^{-1} for 10 min. BIAevaluation software 3.2 RC1 was used for analysis of the data. First, the binding curves for the different dilutions were overlaid and the equilibrium response was determined. Then, the equilibrium response of each experiment was used to create saturation curves of analyte binding and to calculate the dissociation constant (KD) assuming a 1:1 steady state affinity model.

In vitro remodeling of IgG antibodies

The murine anti-TNP IgG1 hybridoma Ab (clone H5) was grown for Ab production in RPMI high glucose (GIBCO) supplemented with 0.03% Primatone RL/UF (Sheffield BioScience) and 1% penicillin/streptomycin. Abs were purified from cell culture media with Protein-G-Sepharose and dialyzed against PBS. *In vitro* galactosylation and/or sialylation was performed in a two-step procedure as described previously[31]. Briefly, 5 mg of Ab were galactosylated by rotating incubation with 75 mU of human β1,4-galactosyltransferase (Calbiochem) and 2 mg of UDP-Galactose (Calbiochem) in 1 ml 50 mM MOPS pH 7.2 with 20 mM MnCl2 for 48 h at 37°C. After buffer exchange to 50 mM MES pH 6.0, IgG was sialylated by incubation with 25 mU of human α2,6-sialyltransferase (Calbiochem) and 0.625 mg of CMP-sialic acid (Calbiochem) for 48h at 37°C. H5 IgG1 was degalactosylated by incubation with ß-galactosidase (10mU) from Prozyme (GK80120) for 48h at 37°C. IgG Abs were separated from enzymes by Protein G chromatography and dialyzing against PBS. Concentrations of the differentially glycosylated IgG1 Abs were determined by BCA-Assays (Pierce) and verified by IgG1 ELISA. Anti-TNP reactivities were measured by ELISA and N-glycosylation of IgG Fc fragments was characterized by MALDI-TOF mass spectrometry.

Determination of IgG1 glycan composition by MALDI-TOF MS

Analysis of N-glycans of IgG samples were performed as previously described[39]. Briefly, tryptic glycopeptides obtained from IgG samples were digested with PNGaseF and the resulting N-glycans were purified by C18 and graphitized carbon columns, permethylated according to standard protocols and analyzed by MALDI-TOF mass spectrometry. Spectra were recorded on an Ultraflex III mass spectrometer (Bruker Daltonics) equipped with a Smartbeam laser and a LIFT-MS/MS facility. Calibration was performed on a glucose ladder and DHB was used as matrix. Spectra were recorded in reflector positive ionization mode and mass spectra from 3000 laser shots were accumulated. The data were evaluated using the GlycoWorkbench software and the Glyco-peakfinder tool.

Förster resonance energy transfer (FRET)

BM neutrophils were stained with Alexa647-labeled anti-Dectin-1 Ab as described above and incubated for 3 min with 1μg ml^{-1} Cy3-labeled HiGal or LoGal H5 IC. Subsequently, cells were fixed using diluted cytofix solution from BD. FRET was measured by determining the fluorescence intensity of the Cy3-HiGal or Cy3-LoGal H5 IC donor before and after photobleaching of the Alexa647 anti-Dectin-1 Ab acceptor. In case of FRET, bleaching the acceptor results in an increase in the fluorescent emission of the donor. Cells were imaged with an Olympus FV1000 (Olympus Europa Holding GmbH, Germany) laser scanning microscope, with a 60 × 1.40 NA oil objective, pinhole diameter was set on automatic, the resolution was set to 320 × 320 pixels at a pixel dwell time of 5 μs. Cy3 was excited at 539 nm, and Alexa Fluor 647 was excited at 635 nm. An image was acquired once before acceptor bleaching and after photodestruction of the Alexa647 label. For

photobleaching, we used the 635nm laser at 50% of the maximum laser power. The bleaching process was monitored in real time and stopped when 100% of photodestruction was achieved. Then, mean fluorescence intensity of Cy3 and Alexa647 was recorded in different regions of interest on the cell surface using Olympus's FV1000 software (Ver. 03.0). The FRET efficiency (E) was calculated as $E = 1 - (I_{DA}/I_D)$, where I_{DA} represents the normalized fluorescence intensity of Cy3 in the presence of nonbleached acceptor. I_D represents the normalized fluorescence intensity of Alexa 647 after complete photodestruction of the acceptor.

Statistical analysis

Statistical analysis was performed using the SigmaStat version 3.5 statistical package (Systat Software). With regard to small sample sizes, normal distribution was assumed. To analyze differences between two normally distributed groups a two-tailed t-test was used. Comparison of the means of more than two normally or non-normally distributed groups was done by one-way analysis of variance (ANOVA) or ANOVA on Ranks. When the mean values of the groups showed a significant difference, pairwise comparison was performed using the Tukey test (ANOVA) or Dunn's method (ANOVA on Ranks). $P < 0.05$ was considered a significant difference. If not stated otherwise, data were taken from 3-5 individual experiments and expressed as mean values ± s.e.m.

Supplementary Material

Refer to Web version on PubMed Central for supplementary material.

Acknowledgments

This work is supported by the German Research Foundation (GRK1727; project 8 and SFB/TR22; project A21) to J.K., EXC306/1 to D.Z, R.L. and J.K., and by DFG EH221-5 to M.E.. P.R.T. is a Medical Research Council (UK) Senior Fellow (G0601617). G.D.B. was supported by the Wellcome Trust. We thank Thies Köhli for technical assistance with the surface plasmon resonance analysis, Thomas Gutsmann for help with the fluorescence spectroscopy measurements, Thomas Peters and Lutz Wollin for helpful discussions and Birgitta Heyman for providing the H5 and the 7B4 hybridoma clones.

References

1. Ricklin D, Hajishengallis G, Yang K, Lambris JD. Complement: a key system for immune surveillance and homeostasis. Nat Immunol. 2010; 11:785–797. [PubMed: 20720586]
2. Klos A, et al. The role of the anaphylatoxins in health and disease. Mol Immunol. 2009; 46:2753–2766. [PubMed: 19477527]
3. Kohl J, et al. A regulatory role for the C5a anaphylatoxin in type 2 immunity in asthma. J Clin Invest. 2006; 116:783–796. [PubMed: 16511606]
4. Hashimoto M, et al. Complement drives Th17 cell differentiation and triggers autoimmune arthritis. The Journal of Experimental Medicine. 2010; 207:1135–1143. [PubMed: 20457757]
5. Rittirsch D, et al. Functional roles for C5a receptors in sepsis. Nat Med. 2008; 14:551–557. [PubMed: 18454156]
6. Markiewski MM, et al. Modulation of the antitumor immune response by complement. Nat Immunol. 2008; 9:1225–1235. [PubMed: 18820683]
7. Clynes R, Dumitru C, Ravetch JV. Uncoupling of immune complex formation and kidney damage in autoimmune glomerulonephritis. Science. 1998; 279:1052–1054. [PubMed: 9461440]
8. Wenderfer SE, et al. C5a receptor deficiency attenuates T cell function and renal disease in MRLlpr mice. J Am Soc Nephrol. 2005; 16:3572–3582. [PubMed: 16207826]
9. Ji H, et al. Arthritis critically dependent on innate immune system players. Immunity. 2002; 16:157–168. [PubMed: 11869678]

10. Shushakova N, et al. C5a anaphylatoxin is a major regulator of activating versus inhibitory FcgammaRs in immune complex-induced lung disease. J Clin Invest. 2002; 110:1823–1830. [PubMed: 12488432]
11. Godau J, et al. C5a initiates the inflammatory cascade in immune complex peritonitis. J Immunol. 2004; 173:3437–3445. [PubMed: 15322209]
12. Nimmerjahn F, Ravetch JV. Fcgamma receptors as regulators of immune responses. Nat Rev Immunol. 2008; 8:34–47. [PubMed: 18064051]
13. Strait RT, Morris SC, Finkelman FD. IgG-blocking antibodies inhibit IgE-mediated anaphylaxis in vivo through both antigen interception and Fc gamma RIIb cross-linking. J Clin Invest. 2006; 116:833–841. [PubMed: 16498503]
14. Jones SL, Knaus UG, Bokoch GM, Brown EJ. Two signaling mechanisms for activation of alphaM beta2 avidity in polymorphonuclear neutrophils. J Biol Chem. 1998; 273:10556–10566. [PubMed: 9553116]
15. Taylor PR, et al. The beta-glucan receptor, dectin-1, is predominantly expressed on the surface of cells of the monocyte/macrophage and neutrophil lineages. Journal of immunology. 2002; 169:3876–3882.
16. Goodridge HS, et al. Activation of the innate immune receptor Dectin-1 upon formation of a 'phagocytic synapse'. Nature. 2011; 472:471–475. [PubMed: 21525931]
17. Taylor PR, et al. Dectin-1 is required for beta-glucan recognition and control of fungal infection. Nat Immunol. 2007; 8:31–38. [PubMed: 17159984]
18. McDonald JU, et al. In vivo functional analysis and genetic modification of in vitro-derived mouse neutrophils. Faseb J. 2011; 25:1972–1982. [PubMed: 21368104]
19. Rogers NC, et al. Syk-dependent cytokine induction by Dectin-1 reveals a novel pattern recognition pathway for C type lectins. Immunity. 2005; 22:507–517. [PubMed: 15845454]
20. Wex E, et al. Induced Syk deletion leads to suppressed allergic responses but has no effect on neutrophil or monocyte migration in vivo. Eur J Immunol. 2011; 41:3208–3218. [PubMed: 21830208]
21. Dennehy KM, Klimosch SN, Steinle A. Cutting edge: NKp80 uses an atypical hemi-ITAM to trigger NK cytotoxicity. Journal of immunology. 2011; 186:657–661.
22. Nimmerjahn F, Ravetch JV. Divergent immunoglobulin g subclass activity through selective Fc receptor binding. Science. 2005; 310:1510–1512. [PubMed: 16322460]
23. Malhotra R, et al. Glycosylation changes of IgG associated with rheumatoid arthritis can activate complement via the mannose-binding protein. Nat Med. 1995; 1:237–243. [PubMed: 7585040]
24. Raju TS. Terminal sugars of Fc glycans influence antibody effector functions of IgGs. Curr Opin Immunol. 2008; 20:471–478. [PubMed: 18606225]
25. Geijtenbeek TB, Gringhuis SI. Signalling through C-type lectin receptors: shaping immune responses. Nat Rev Immunol. 2009; 9:465–479. [PubMed: 19521399]
26. Barb AW, Prestegard JH. NMR analysis demonstrates immunoglobulin G N-glycans are accessible and dynamic. Nat Chem Biol. 2011; 7:147–153. [PubMed: 21258329]
27. Wernersson S, et al. IgG-mediated enhancement of antibody responses is low in Fc receptor gamma chain-deficient mice and increased in Fc gamma RII-deficient mice. J.Immunol. 1999; 163:618–622. [PubMed: 10395649]
28. Sitaru C, et al. Induction of dermal-epidermal separation in mice by passive transfer of antibodies specific to type VII collagen. J Clin Invest. 2005; 115:870–878. [PubMed: 15841176]
29. Yoshitomi H, et al. A role for fungal {beta}-glucans and their receptor Dectin-1 in the induction of autoimmune arthritis in genetically susceptible mice. The Journal of Experimental Medicine. 2005; 201:949–960. [PubMed: 15781585]
30. Manicassamy S, et al. Toll-like receptor 2-dependent induction of vitamin A-metabolizing enzymes in dendritic cells promotes T regulatory responses and inhibits autoimmunity. Nat Med. 2009; 15:401–409. [PubMed: 19252500]
31. Anthony RM, Wermeling F, Karlsson MC, Ravetch JV. Identification of a receptor required for the anti-inflammatory activity of IVIG. Proc Natl Acad Sci U S A. 2008; 105:19571–19578. [PubMed: 19036920]

32. Arnold JN, Wormald MR, Sim RB, Rudd PM, Dwek RA. The impact of glycosylation on the biological function and structure of human immunoglobulins. Annu Rev Immunol. 2007; 25:21–50. [PubMed: 17029568]
33. Agarwal S, Cunningham-Rundles C. Autoimmunity in common variable immunodeficiency. Curr Allergy Asthma Rep. 2009; 9:347–352. [PubMed: 19671377]
34. Otto M, et al. C5a mutants are potent antagonists of the C5a receptor (CD88) and of C5L2: position 69 is the locus that determines agonism or antagonism. J Biol Chem. 2004; 279:142–151. [PubMed: 14570896]
35. Nimmerjahn F, Ravetch JV. Analyzing antibody-Fc-receptor interactions. Methods Mol Biol. 2008; 415:151–162. [PubMed: 18370153]
36. Graham IL, Anderson DC, Holers VM, Brown EJ. Complement receptor 3 (CR3, Mac-1, integrin alpha M beta 2, CD11b/CD18) is required for tyrosine phosphorylation of paxillin in adherent and nonadherent neutrophils. J Cell Biol. 1994; 127:1139–1147. [PubMed: 7525604]
37. Wang GG, et al. Quantitative production of macrophages or neutrophils ex vivo using conditional Hoxb8. Nat Methods. 2006; 3:287–293. [PubMed: 16554834]
38. Rosas M, et al. The induction of inflammation by dectin-1 in vivo is dependent on myeloid cell programming and the progression of phagocytosis. J Immunol. 2008; 181:3549–3557. [PubMed: 18714028]
39. Wedepohl S, et al. N-glycan analysis of recombinant L-Selectin reveals sulfated GalNAc and GalNAc-GalNAc motifs. J Proteome Res. 2010; 9:3403–3411. [PubMed: 20469932]

Europe PMC Funders Author Manuscripts

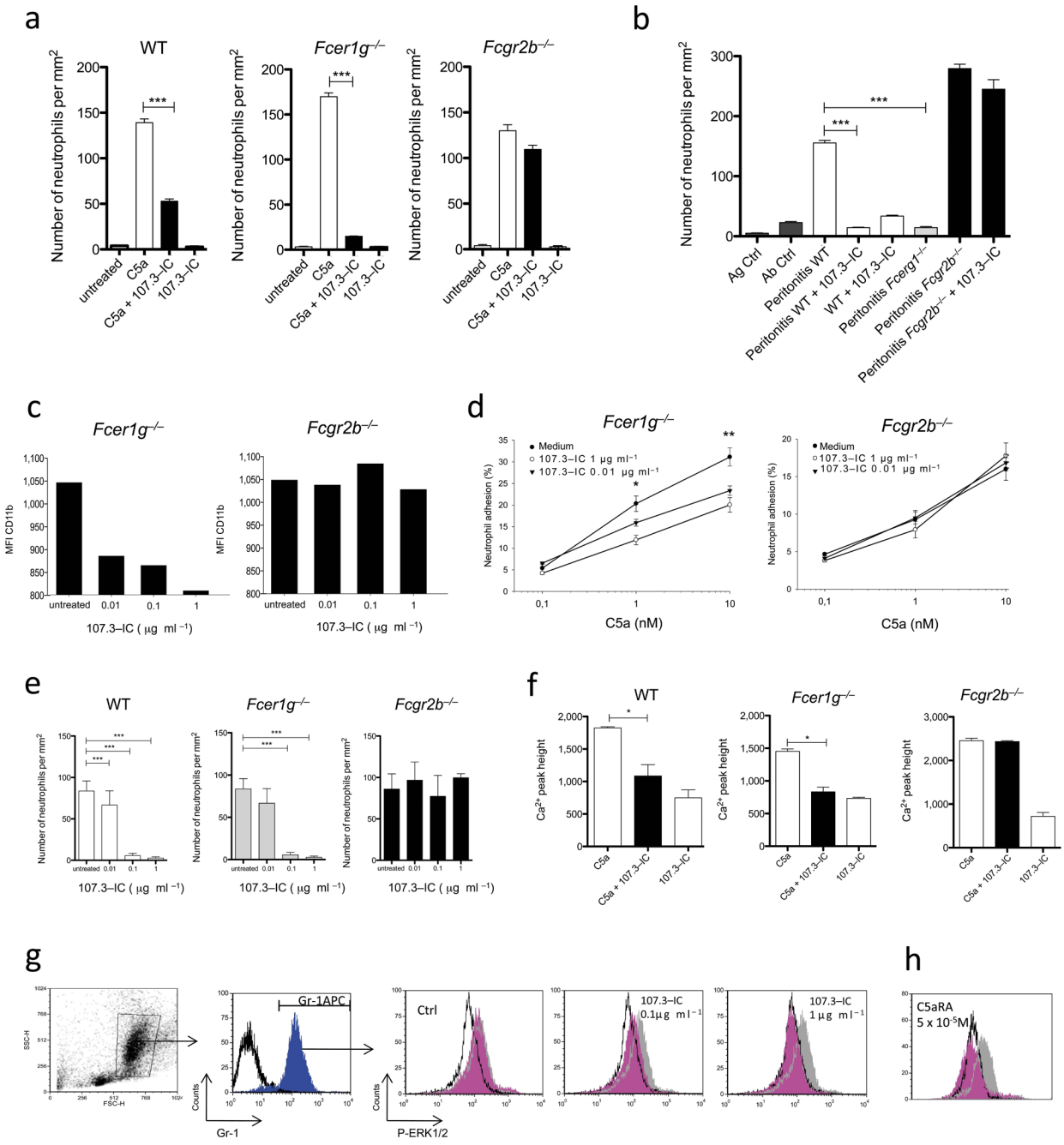

Figure 1. IgG1 immune complexes (IC) inhibit C5a-mediated inflammatory responses in vivo and in vitro by an FcγRIIB-dependent mechanism

Peritoneal migration of neutrophils in response to C5a (**a**) or OVA/anti-OVA-IC (**b**) ± 107.3-IC in WT, *Fcer1g*$^{-/-}$ or *Fcgr2b*$^{-/-}$mice. Impact of 107.3-IC on **(c)** CD11b expression and (**d**) iC3b-dependent adhesion in neutrophils from *Fcer1g*$^{-/-}$ and *Fcgr2b*$^{-/-}$ mice. C5a-mediated migration of BM-derived neutrophils (**e**) and increase in $[Ca^{2+}]_i$ in BM-derived cells (**f**) in WT, *Fcer1g*$^{-/-}$ or *Fcgr2b*$^{-/-}$ mice ± 107.3-IC. (**g**) Gating of BM neutrophils according to their FSC/SSC pattern (left dot-plot) and the expression of the Gr-1 marker (1st histogram on the left). Dose-dependent impact of 107.3-IC on C5a-mediated ERK1/2 phosphorylation in Gr-1^{+} WT BM neutrophils. (**h**) Effect of a C5a receptor antagonist

(C5aRA) on C5a-mediated ERK1/2 phosphorylation. White histogram: ERK phosphorylation in the absence of C5a (background); grey histogram: treatment with C5a (5×10^{-7}M; 1 min); magenta histogram: C5a (5×10^{-7}M; 1 min) ± 107.3 IC (**g**) or C5aRA (**h**) at the indicated concentrations. Results in (**c**) and (**g**) are representative of at least three independent experiments. Values in (**a**) and (**b**), and (**d-f**) are means ± s.e.m. (n=5-10/group). *P<0.05, **P<0.01, ***P<0.001.

Europe PMC Funders Author Manuscripts

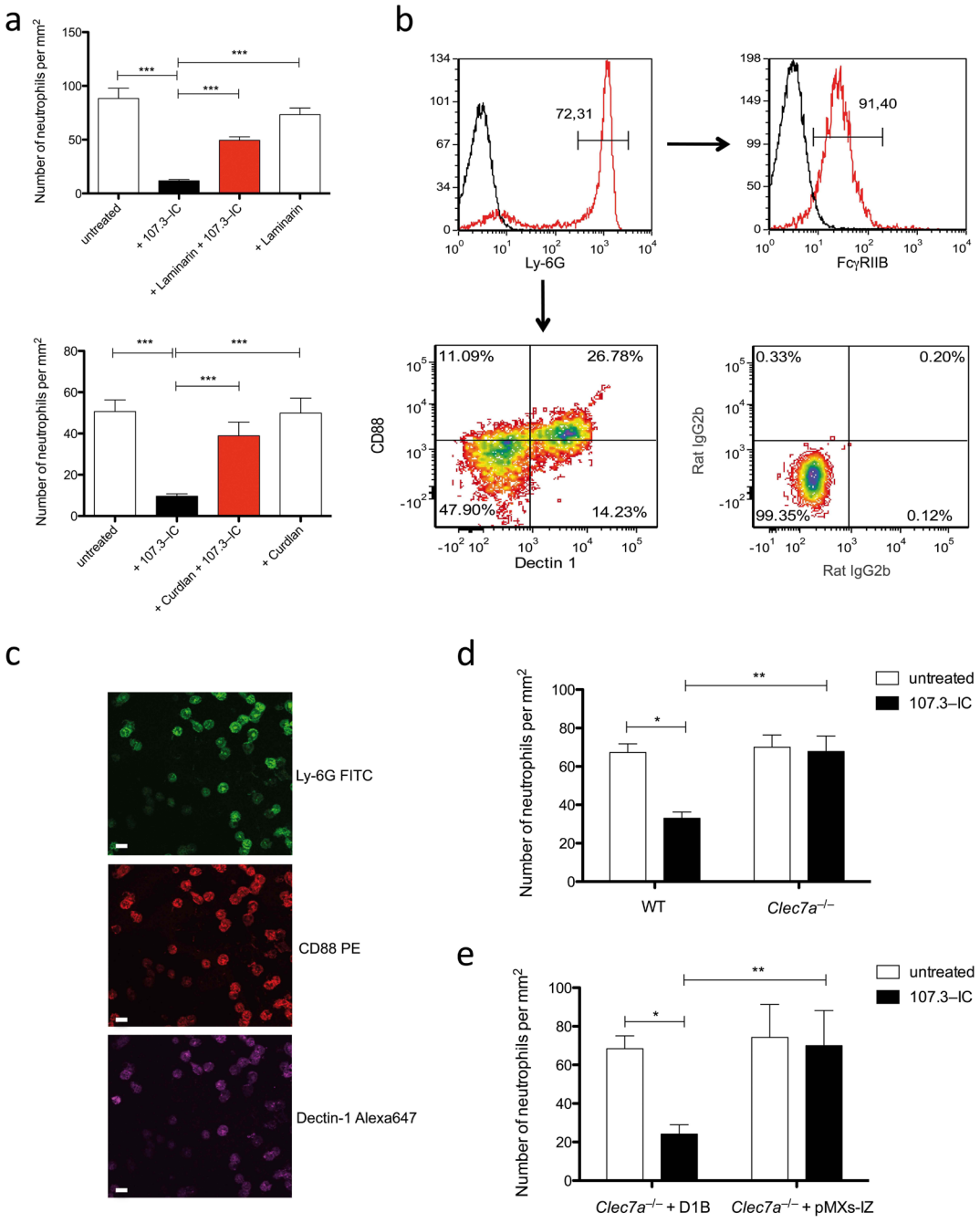

Figure 2. The inhibitory effect of IgG1 IC depends on Dectin-1

(**a**) Impact of 107.3-IC on C5a-mediated migration of BM neutrophils when Dectin-1 is blocked by laminarin (upper panel) or curdlan (lower panel) (n=3/group). (**b**), C5aR(CD88) and Dectin-1 expression (lower left contour-plot; isotype control shown in the lower right plot) on Ly-6G^{hi} BM-derived neutrophils (upper left histogram) as determined by flow cytometry. FcγRIIB expression of Ly-6G^{hi} neutrophils is shown in the upper right histogram. (**c**) BM cells that migrated towards C5a (10^{-8} M for 30 min) were stained on the membrane for expression of Ly-6G, Dectin-1 and C5aR and analyzed by confocal microscopy. All migrated cells are Ly-6G^{hi} neutrophils that express Dectin-1 and C5aR.

Impact of 107.3-IC treatment on C5a-mediated chemotaxis of (**d**) BM-derived neutrophils from 129 wt and from *Clec7a*$^{-/-}$ mice or (**e**) a *Clec7a*$^{-/-}$ neutrophil cell line transfected with the Dectin-1B isoform (D1B) or with vector alone (pMXs-IZ) (**d** and **e**, n=3/group). Values are means ± s.e.m. *P<0.05, *P<0.01, *** P<0.001.

Europe PMC Funders Author Manuscripts

Europe PMC Funders Author Manuscripts

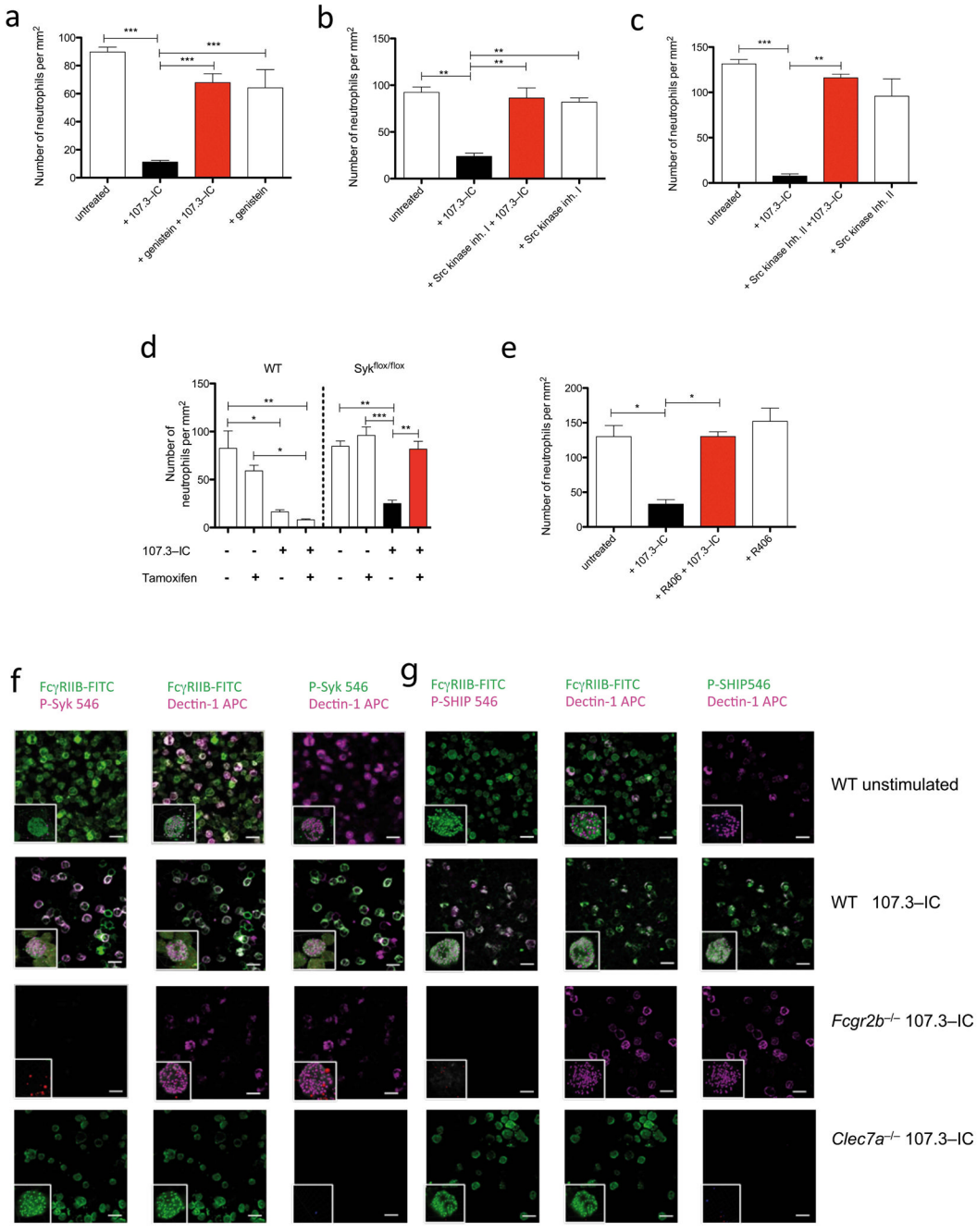

Figure 3. IgG1 IC activate Src kinase and promote phosphorylation of tyrosine and Syk downstream of Dectin-1 and of SHIP downstream of FcγRIIB

C5a-mediated chemotaxis of BM neutrophils ± 107.3-IC in the presence or absence of (**a**) specific blockade of tyrosine phosphorylation by genistein, (**b**) Src kinase inhibitors I or (**c**) II. (**d**) C5a-mediated chemotaxis of BM neutrophils in cells from conditional Syk knockout mice ($Syk^{flox/flox}$) ± tamoxifen treatment. (**e**) Impact of the Syk tyrosine kinase blockade by R406 on C5a-mediated BM neutrophil chemotaxis in the presence of 107.3-IC. Values in (**a-c** and **e**) are means ± s.e.m.(n=3-5/group). *P<0.05, **P< 0.01, ***P<0.001. (**f, g**) Impact of 107.3-IC treatment on phosphorylation of (**f**) Syk (p-Syk) or (**g**) SHIP (p-SHIP) in BM-neutrophils from WT, *Fcgr2b*$^{-/-}$ or *Clec7a*$^{-/-}$ mice. Depicted are immunofluorescence

signals in the absence of 107.3 IC (1st rows in **f** and **g**) or obtained 3 min after incubation with 107.3 IC (2nd - 4th rows in **f** and **g**). Co-localization of P-Syk and p-SHIP with FcγRIIB and Dectin-1 in response to 107.3 IC treatment is evidenced by white fluorescent neutrophils in the 2nd row of (**f**) and (**g**). The inserts show co-localization (white spots) using z-stacks of images acquired by confocal microscopy and isosurfaced using the IMARIS image analysis software. Results are representative of two (*Clec7a*$^{-/-}$) or three independent experiments.

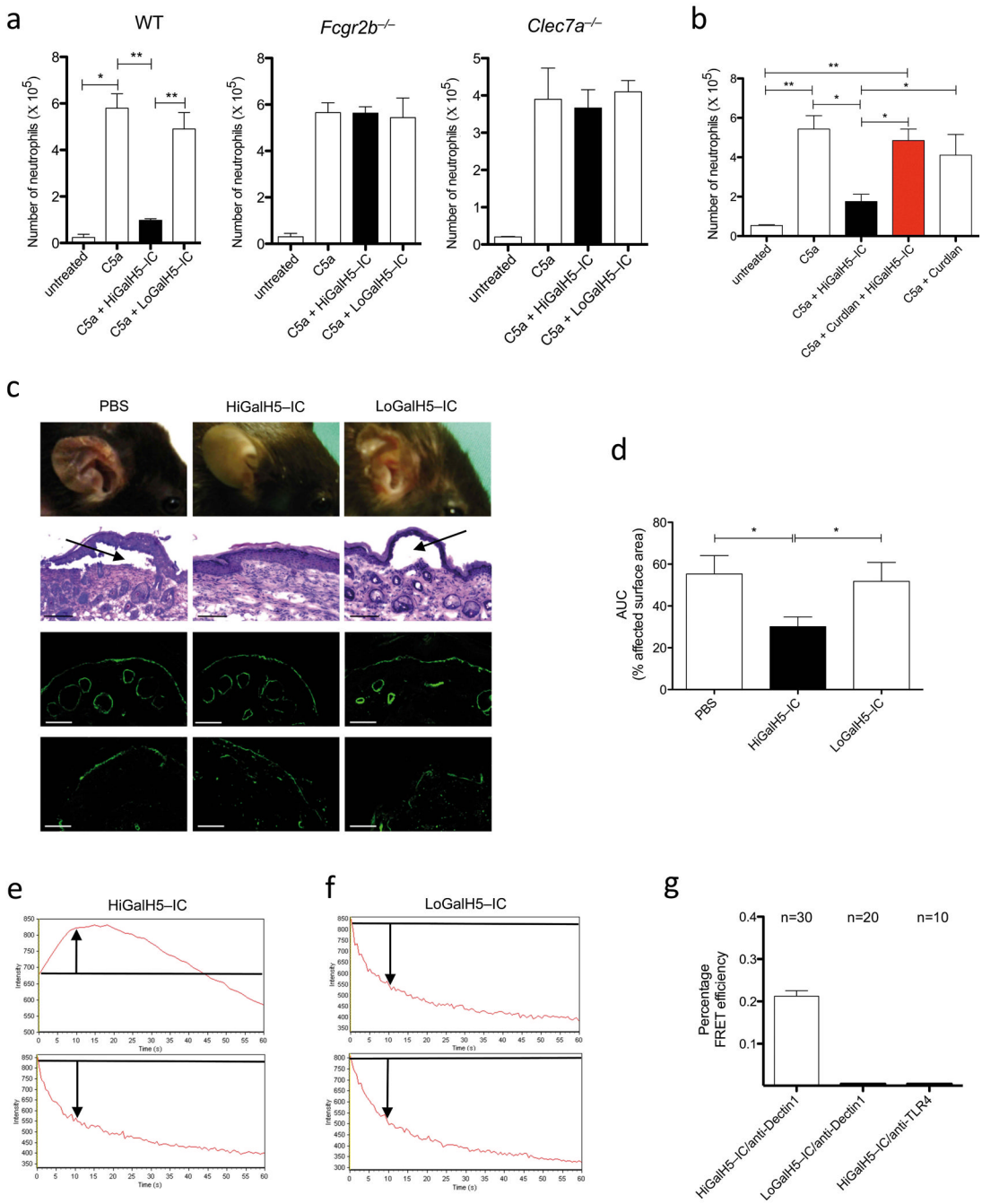

Figure 4. High Fc glycan galactosylation is critical for the inhibitory effect of Ig1 IC in vivo and drives the association of FcγRIIB and Dectin-1

(**a**) Peritoneal migration of neutrophils in response to C5a ± 107.3-IC in WT, *Fcgr2b*$^{-/-}$ or *Clec7a*$^{-/-}$ mice. (**b**) Impact of curdlan pretreatment on peritoneal neutrophil migration in response i.p injection of C5a ± HiGalH5-IC. (**c**) Development of cutaneous lesions (1st row), subepidermal split formation (2nd row), linear deposition of rabbit anti-type VII collagen (3rd row) and C3 (4th row) at the basement membrane in experimental EBA (d 12) in the PBS, HiGalH5- and LoGal-H5-IC treatment groups. Black arrows point towards dermal-epidermal separation. Scale bars, 100μm. (**d**) Clinical disease severity in the PBS, LoGalH5- and HiGalH5-IC-treated animals during the course of experimental EBA (d 4-12) as

Europe PMC Funders Author Manuscripts

quantified by assessment of the area under the curve (AUC); values in (**a**), (**b**) and (**d**) are means ± s.e.m. **P*<0.05, ***P*<0.01. (**a** and **b**, (*n*=5/group), (**c**, *n*=9-12/group). Time dependent change in fluorescence intensity of Cy3-HiGal- (**e**) and Cy3-LoGalH5-IC (**f**) during acceptor photobleach in the presence (top pictures) or absence (bottom pictures) of acceptor staining on BM cells. Arrows indicate the change of fluorescence intensity as compared with the starting value (marked by the black line). (**g**) FRET efficiency following acceptor bleaching in BM cells treated with either Cy3-HiGalH5- or Cy3-LoGalH5-IC as donor and anti-Dectin-1 $Ab^{Alexa647}$ as acceptor. As a negative control, Cy3-HiGalH5-IC was used as donor and anti-TLR4 $Ab^{Alexa647}$ as acceptor. *n*=number of cells evaluated.